Exp Brain Res (2001) 137:369–386
DOI 10.1007/s002210000667

RESEARCH ARTICLE

H.L. Galiana · H.L.H. Smith · A. Katsarkas

Modelling non-linearities in the vestibulo-ocular reflex (VOR) after unilateral or bilateral loss of peripheral vestibular function

Received: 22 February 2000 / Accepted: 6 December 2000 / Published online: 1 March 2001

Abstract We recorded the vestibulo-ocular reflex (VOR) in 18 normal subjects, 50 patients with unilateral loss of vestibular function and 18 patients with bilateral loss of vestibular function. The unilateral cases had either partial loss (i.e. vestibular neuronitis or Meniere's disease) or total loss (i.e. vestibular nerve section), whereas bilateral cases had only partial loss (i.e. due to ototoxicity or to suspected microangiopathy, secondary to severe kidney disease). Tests were performed at 1/6-Hz passive head rotation in the dark, with peak head velocities ranging from 125 to 190°/s. We report on the distinct VOR non-linearities observed in unilateral versus bilateral patients: whereas unilateral patients all exhibit an *asymmetric* hypofunction with *decreasing* VOR gain at higher head velocities, bilateral patients have a more severe but *symmetric* hypofunction associated with *increasing* VOR gain at higher head velocities. We present a model study that can duplicate the nature of these characteristics, based mainly on peripheral non-linear semicircular canal characteristics and secondary central compensation. Theoretical analyses point to the importance of clinical test parameters (rotation speed and frequency) in the determination of a functional VOR and the detection of reflex non-linearities, so that test protocols can seriously bias the evaluation of adequate functional recovery.

Keywords Vestibular loss · Unilateral · Bilateral · Nystagmus · Compensation

H.L. Galiana (✉) · H. L. H. Smith
Department of Biomedical Engineering, McGill University,
3775 University St., Rm 308, Montreal, Québec H3A 2B4,
Canada
e-mail: mimi@bmed.mcgill.ca
Tel.: +1-514-3986738, Fax: +1-514-3987461

A. Katsarkas
Department of Otolaryngology,
McGill University and Royal Victoria Hospital, Montreal,
Québec H3A 2B4, Canada

Introduction

The vestibulo-ocular reflex (VOR) provides compensatory involuntary eye movements, such that the eyes are stabilised on a spatial goal during unexpected head movements. The observed ocular response normally alternates between slow and fast phases to form so-called vestibular nystagmus. We will focus on the horizontal VOR, measured in the dark during passive whole-body rotation around a vertical axis. The main compensatory role of the VOR is realised during slow phases, where the eye(s) move(s) in the opposite direction to the head to maintain a near-constant viewing direction in space. Fast phases are intermittent, quickly redirecting the eye, usually in the direction of the head movement (anti-compensatory), in order to allow the eye to stabilise gaze at a new position in space. The properties of VOR slow phases have been reported in the literature by several groups in both normal subjects and in patients suffering from *unilateral* vestibular deficits (Hain et al. 1987; Baloh et al. 1989; Paige 1989; Katsarkas et al. 1995). Patients are typically found to have reduced linear ranges in the VOR and to exhibit asymmetries in the gain when comparing responses towards and away from the lesion. Steadily decreasing sensitivities, which eventually reach a saturated response, are also found with increasing rotation speeds towards the lesion. We report similar results below, with the addition of observations from patients with *bilateral* vestibular deficits. In the latter case, the nature of the VOR non-linearities is found to be *opposite* to that of unilateral patients: the VOR sensitivity (gain) is low, but now *increases* symmetrically with larger head speeds in either direction. This paper presents the experimental data and provides a simple peripheral explanation for the discordant nature of the non-linearities, using simulations in a bilateral, non-linear model of the VOR.

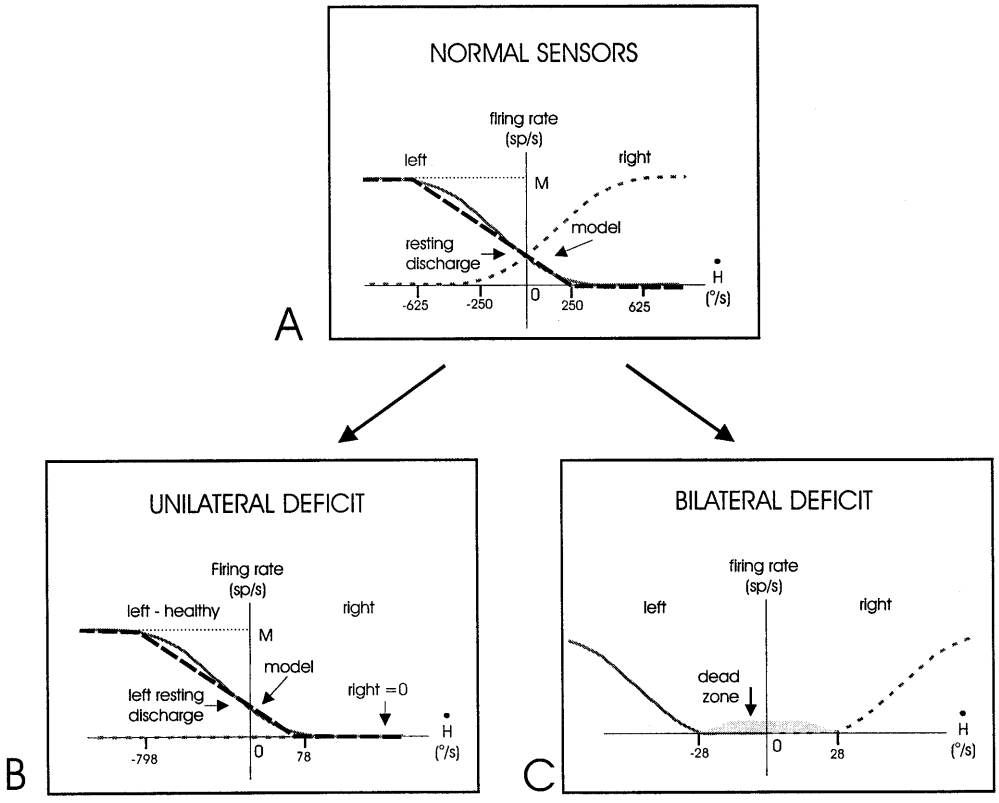

Fig. 1A–C Plots of canal sensitivity to head velocity, with approximations used in the models. (See Tables 4 and 5 for values of M saturation and resting rates.) **A** Linear models in normal subjects; **B** after right unilateral nerve section, linear with reduced bias; **C** in bilateral patients, non-linear canals with dead-zone. Functional ranges are presented with respect to head velocity. *M* Saturation level, *H* head velocity

Background

First, a brief review of the physiological substrates for vestibular nystagmus is provided, which implies the need for modelling VOR responses throughout nystagmus. There are three main components: the semicircular canals, the central neural pathways and the ocular motor system (eye muscles and eyeballs). Non-linear properties at any of these levels can distort the VOR and invalidate the use of a lumped dedicated model for the compensatory VOR (slow phases alone).

Central and behavioural observations appear remarkably linear during VOR slow phases, due to several factors. First, thanks to nystagmus during head rotations, eye positions remain well within motor limits in the orbit, ~50° in man and monkeys (Barnes 1980; Baker et al. 1981; Laurutis and Robinson 1986; Tomlinson and Bahra 1986). Second, the same nystagmus causes many premotor activities during slow phases to modulate further away from cut-off or saturation (e.g. Scudder and Fuchs 1992) due to central response components related to eye position. Theoretical studies have demonstrated that the action of such nystagmus, in a bilateral structure can be a major factor in extending the linear range of the VOR, despite potential limitations of low background activities at sensory and central levels (Galiana 1991; Smith and Galiana 1991). Nystagmus, therefore is a plausible mechanism for observations that the VOR is much more linear than its primary sensors (Laurutis and Robinson 1986; Tomlinson and Bahra 1986).

Finally, it is known that the generation of horizontal nystagmus is associated with the activation of burst cells in the reticular formation (Henn et al. 1982; see Galiana 1991 for a full discussion) and the silencing or severe inhibition of many premotor vestibular cells ipsilateral to the fast phase direction. This is clearly a form of functional structural modulation. Hence, even though nystagmus supports linear function in the VOR, lumped linear models for studying VOR slow phases in isolation are still not justified. As explained elsewhere (Galiana and Outerbridge 1984; Galiana 1991), constant switching between modes can affect the *dynamics* (time constants) estimated from slow-phase VOR envelopes (linked slow-phase segments) and the shape of measured non-linearities. In conclusion, despite some functional linearities, VOR-data interpretation must always be linked to bilateral models of both slow and fast phases, in order to allow consistency in parameter estimates.

Primary characteristics

Regular primary afferents from the canals are the likely dominant input for the rotational VOR (Minor and Goldberg 1991; Chen-Huang et al. 1997). They are known to have an asymmetric sensitivity, preferring ipsilateral to contralateral head rotation, especially at low rotation frequencies or during steps of acceleration (Paige 1989; Goldberg and Fernandez 1971). In addition, the primary sensitivity measured during steps of acceleration is a

function of the applied stimulus level (e.g Brichta and Goldberg 2000). Like all neural responses, primary activity is also limited by cutoff and saturation levels (Segal and Outerbridge 1982). The canal sensitivity to head velocity at a particular frequency is, therefore, dependent on the amplitude and direction of input stimuli, which can be represented as a non-linear sigmoidal curve (Fig. 1A). However, the *degree* of non-linearity observed at various rotational frequencies will additionally vary because of the *dynamics* of sensory-neural transduction (see Discussion): for example, in the *healthy case* at 1/6 Hz, we demonstrate that primary non-linear characteristics are well described by a simple straight line (dashed line in Fig. 1A), limited by cut-off and saturation levels (see also the Methods section).

Such non-linear dynamic sensors, with reciprocal characteristics, can cause a functional increase in the linear range of a reflex when projecting onto a symmetric (bilateral) premotor system (Smith and Galiana 1991). Hence, an adequate study of the non-linear properties of the VOR, with or without peripheral deficits, requires bilateral representations of *both* sensors and premotor circuits, as well as a representation of nystagmus effects.

Summary

This paper investigates the effects of unilateral or bilateral losses in the vestibular apparatus on sinusoidal rotation tests of the VOR performed in the dark. The unilateral and bilateral loss data is then compared with that of normal subjects. Data from normal subjects and patients with unilateral losses, together with our analysis procedures, have been presented in part previously (Smith et al. 1997; Katsarkas et al. 1998). Here, we add the unusual properties of the VOR in bilaterally lesioned patients. By focusing on a representative case from each group, the various non-linear properties of the VOR are explained using simulations of a bilateral non-linear model of sensory and central VOR pathways (see Methods section). The model includes switching of pathways to implement the generation of nystagmus, since this can affect the observed VOR dynamics and linearity.

Materials and methods

Acquisition of human data

This study included 18 normal subjects, 50 patients with unilateral loss of vestibular function and 18 patients with bilateral loss of vestibular function, as determined by caloric tests. The unilateral cases had either partial loss (i.e. vestibular neuronitis or Meniere's disease) or total loss (i.e. vestibular nerve section), whereas bilateral cases had severe loss (i.e. due to ototoxicity or suspected microangiopathy secondary to severe kidney disease). Control subjects were considered normal if they had no history of dizziness, ear or neurological disease. Patients were from the Dizziness Clinic at the Royal Victoria Hospital in Montreal, Canada, under the care of one of us (A.K.). According to history and neurology assessment, the patients had no detectable brainstem problems. All experiments had ethics committees' approval.

Silver/silver-chloride electrodes were used to record conjugate eye position in the horizontal plane. All subjects remained in dim red light for 20 min and were then seated on a servo-controlled rotating chair, restrained by seat belts and a head holder. The head and body were fixed en-bloc to the chair during rotations in the dark, while subjects were instructed to perform mental arithmetic. All experimental protocols used a sequence of sinusoidal rotations at 1/6 Hz, with increasing peak head velocities (typically ~125, 160 and 190°/s). This was done to explore the sensitivity of VOR biases and non-linearities to stimulus amplitude, thereby assisting in determining the cause of the non-linearities (Galiana et al. 1995; Katsarkas et al. 1995). Each test lasted 52 s, of which the last 32 s were recorded to measure VOR properties in steady state. Full electrooculogram (EOG) calibrations were performed before and after the sequence of rotations, and offsets (null position) were re-measured between the rotation tests to control for electrode drift.

The chair was controlled by a Pentium computer, using software developed in house with Modula-2 (Jensen Partners International, Mountain View, Calif., USA). Eye position and head (chair) position channels underwent analogue low-pass filtering (8-pole Bessel) to 40 Hz to avoid aliasing when sampled. Data were recorded on separate channels of a 16-bit National Instruments A/D board and stored at 500 Hz for later analysis. Signal processing was carried out off-line on a Pentium using software developed locally with Matlab (Mathworks, Natwick, Mass., USA). The sampled signals were digitally low-pass filtered down to 15 Hz and then decimated to a 100-Hz sampling rate to save storage space. This 15-Hz bandwidth was sufficient to examine the slow-phase characteristics, in spite of mild distortions on the fast-phase trajectories.

The position traces were digitally differentiated to obtain eye and head velocity trajectories and scanned by our classification algorithm to demark slow-phase segments automatically (Rey and Galiana 1991). The extracted slow-phase data were then examined visually in X-Y plots (see Results) and computationally by fitting appropriate linear or cubic descriptions to the VOR characteristics. As described in detail elsewhere (Katsarkas et al. 1995), this required first removing any phase shift (dynamics) between the stimulus and response curves. Justification for the selection of a linear or cubic model was done on the basis of the associated variance-accounted-for and BIC to avoid over-modelling (Galiana et al. 1995). VOR characteristics were modelled by the expressions in Eq. 1, where y represents the slow-phase eye velocity, and x represents the phase-shifted head velocity in a particular sinusoidal protocol. Parameter estimates were obtained by regression with experimental data.

$$\begin{aligned}&\text{linear fit: } y=m+nx\\&\text{cubic fit: } y=m+nx+px^2+qx^3\\&\text{model selection criteria: BIC}=\log(mse)+\log(N)\cdot P/2N\\&\text{quality of fit: VAF}=100\cdot(1-mse/\text{variance of data})\end{aligned} \quad (1)$$

In both linear and cubic cases, the linear gain term (n) defines the VOR sensitivity for low-velocity rotations, and the dc offset (or bias) is the zero-order coefficient (m). P is the number of model parameters (two for linear, four for cubic), N is the number of data points in the pooled slow phases and mse is the mean square error of the fit $[\Sigma^{N}_{j=1}\{\text{eye}(j)-y(j)\}^2/N]$. In the case of normal subjects, a straight line fit the data well, while for patients a curve was often necessary (Baloh et al. 1989; Paige 1989; Galiana et al. 1995; Katsarkas et al. 1995). The quality of the fit is assessed by the variance-accounted-for (VAF), a percentile figure similar to the squared regression coefficient in standard linear regression.

VOR simulations

Simulations were performed to replicate the responses found in unilateral patients as well as the unusual responses found in most bilateral patients. A model simulating the bilateral VOR anatomy was first proposed by Galiana and Outerbridge (1984) and further discussed in Galiana (1991) and Smith and Galiana (1991). It is

reproduced in the Appendix as Simulink formulations for ease of reference [Figs. 12 (slow phases) and 13 (fast phases)]. Tables are also provided in Appendix A for model parameters used in the three simulation cases presented in the Results. The VOR model relies on a simple first-order representation of the eye plant. Limitations on neural firing rates at all levels are implemented by rectification/saturation at all summing junctions ("cells"). The dynamics of the sensors (canals) on both sides are more complicated. One must consider both the high-pass dynamics and the non-linear (asymmetric) sensitivities of the transduction process, as mentioned above.

The geometric properties of the semicircular canals cause bending of the cupula approximately in phase with head velocity at rotational frequencies above ~0.1 Hz (time constant ~4 s). Next, the mechano-neural transduction process has non-linear properties causing asymmetric changes in firing rate on the primary afferents, sensitive to both the direction and speed of the head. This can be expressed by the following equation, relating primary activity, C(S), with associated head velocity, H_v(s), in the Laplace domain:

$$\mathbf{C}(S)=k\{H_v\}\cdot[\boldsymbol{H_v}(S)\cdot T_1S/(T_1S+1)]+R_c/S \quad (2)$$

where S is the Laplace variable, and bold-face type indicates transform of the variables:

- T_1 = Canal time constant, s
- R_c = Canal resting rate, sp/s
- H_v = Head velocity, degrees/s
- k = Canal sensitivity with respect to head velocity (slopes in Fig. 1), itself a function of head velocity amplitude in the non-linear case.

Note the order of the operations: dynamics must be applied to head velocity *before* the non-linear gain k, since cupula bending then causes neural activation. If the order of operations is reversed in a non-linear system, the result is not the same (non-commutative).

The sensitivity of the *healthy* canal (k, slope of dashed line in Fig. 1) is represented in the model with a simple straight line, with non-zero intercept, so that the canal primary activity is biased at R_c sp/s with a stationary head. For our 1/6-Hz protocols, this linear assumption is justified in the Discussion. In those lesion cases where a non-linear canal was deemed necessary to duplicate data (e.g. Fig. 1C), the canal sensitivity was described by a quadratic function of concurrent head velocity, as a simple approximation for a sigmoidal curve; e.g. for the right canal this would be evaluated from

$$k=aH_v^2+bH_v \quad (3)$$

The choice of {a,b} pairs can change the shape of the effective canal transduction process. The relevant k description is substituted in Eq. 2, so long as C(S) is positive and less than some desired saturation level (M). If C(S) exceeds these limits, it is fixed at zero or M=350 sp/s, as appropriate (see Fig. 1). These 0-M limitations on the firing rates are applied at all levels in the central VOR circuit. The expression for the left canal uses Eq. 2 with H_v replaced by $-H_v$ (opposite sensitivity).

For the purposes of this paper, we have also added an initial central processing stage (not in Galiana 1991; Galiana and Outerbridge 1984) to provide improvement on the apparent vestibular time constant (velocity storage), even when gaze holding is excellent. The phase angle, between head velocity and corresponding slow-phase eye velocity, is affected by canal dynamics and by any central processors. The canal time constant, T_1 in Fig. 12, is determined by the physical structure of the canal (4–6 s). However, the range of VOR phase angles observed in our data cannot come from T_1 alone. In previous papers, it was shown that a behavioural improvement on the canal-time constant could appear without a velocity storage stage, depending on the goals of fast phases and the transient effects of switching (Galiana 1991; Mettens et al. 1994). This nystagmus-driven shaping of the slow phase is only effective if the time constant of gaze holding is less than 1–2 s or if the stimulus is of very low bandwidth (e.g. a step). In such cases, significant discontinuities in eye-velocity levels should appear across fast-phase intervals (end of one slow-phase relative to beginning of next slow-phase). Our normal subjects and some patients had good gaze holding and, yet, still showed VOR time constants larger than expected from the primaries (smaller phase leads) at the experimental test frequency of 1/6 Hz. Since these subjects had smooth transitions between slow-phase eye velocities during nystagmus, this implied a healthy (large) gaze-holding capacity, and switching dynamics could not play a role in improving VOR phase. Hence, we had to include a bilateral stage to pre-process signals on vestibular afferents, akin to that proposed by Hain et al. (1987). This initial stage normally causes an apparent increase in the effective vestibular time constant at the behavioural level (velocity storage), though the *opposite* can also be realised by appropriate selection of parameters (see patient sections below).

Simulated data was produced by implementing the bilateral model with Simulink (Mathworks, Natwick, Mass., USA) on a Pentium, at a sampling rate of 0.01 s. The simulations were repeated for three cases; under normal conditions with two intact linear canals, with one modified canal (unilateral peripheral lesion) and, finally, with two modified canals (bilateral case). The same Simulink models for slow and fast phases were used in all cases (Figs 12 and 13 in Appendix), with simple parametric adjustments for each condition. These parametric changes are explained in the Results section and tabulated in the Appendix for the three representative cases. Finally, the simulated results underwent the same analysis procedure as the experimental data, to compare measured versus simulated behaviour (gain, phase, non-linearity, bias).

Results

Experimental measurements of the human VOR and simulations of this reflex were all performed at various peak head velocities (see Methods) at a fixed oscillation frequency of 1/6 Hz. This was done to verify consistency between data and simulations not only in a given protocol, but also across protocols in a given subject. In general, characteristics associated with increasing peak head velocity in a protocol confirm previous work (e.g., Katsarkas et al. 1995) and are reproduced by model simulations. These include observed increases in fast-phase rate with peak head velocity, a variable VOR bias moving towards the lesioned side with protocol speed and smoothing of VOR non-linearities observed at low test speeds. Here, we will focus the presentation on results during the protocol with the highest rotation speed, in the interest of space. The main goal here is to find a common mechanism to explain the diverse VOR characteristics, which appear with different peripheral vestibular lesions.

Experimental observations of the VOR

Normal cases

When relating VOR slow-phase eye velocity to head velocity, the VOR phase lead of 18 normal subjects examined so far was usually small, as computed from the optimal time shift required to "collapse" the x-y plot of head velocity with respect to eye velocity. The resulting VOR

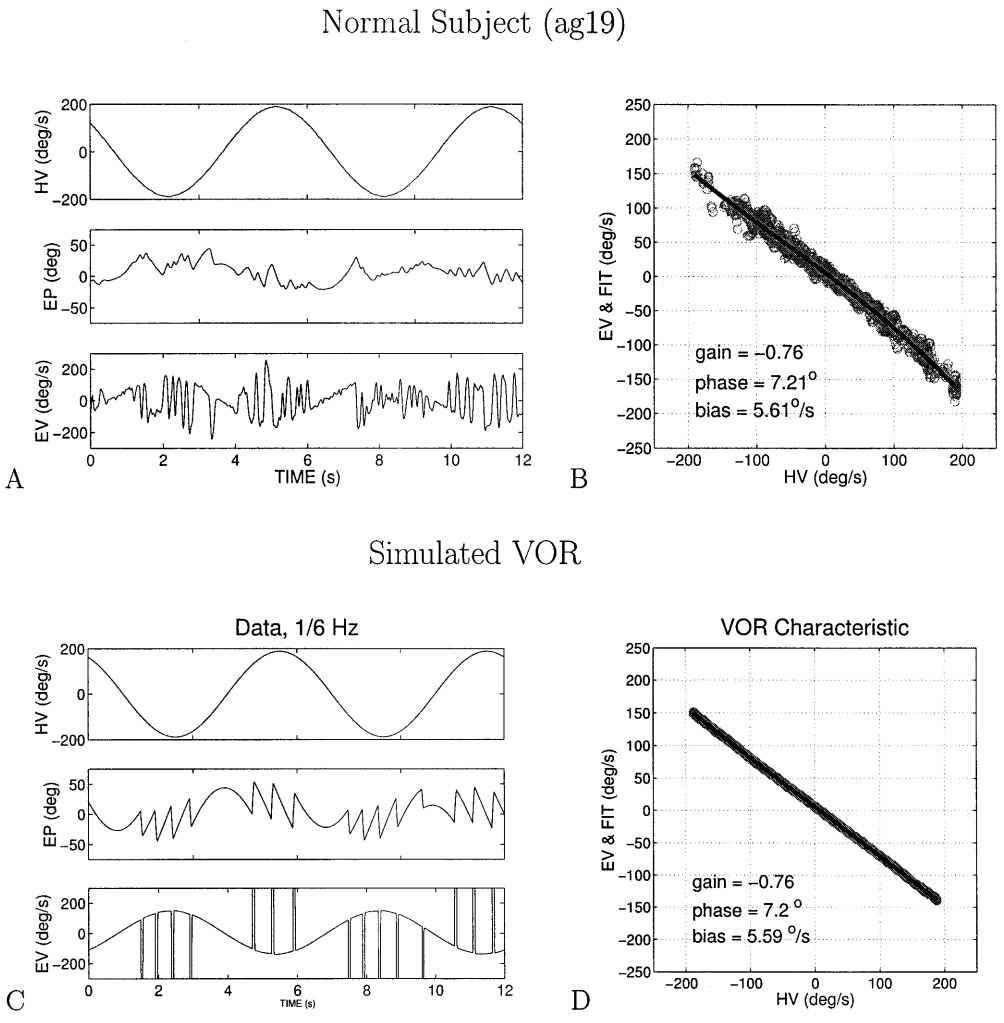

Fig. 2A–D Data for a normal subject (ag19). **A** Vestibulo-ocular-reflex (*VOR*) data time plots of head velocity (*HV*), eye position (*EP*) and eye velocity (*EV*). Positive values correspond to rightward direction. **B** Slow-phase eye velocity versus head velocity with the phase lead removed and superimposed polynomial fit (*bold curve*). **C** Simulation of this VOR data. **D** X-Y plot, as in **B** above, for the simulation data. *Inserts* in **C** and **D** provide the estimates of gain, phase and bias in the real and simulated data

Table 1 Sample vestibulo-ocular reflex characteristics in normal subjects (see Eq. 1 for definitions)

Subject	Cubic (q)	Quadr. (p)	Gain (n)	Bias (m, °/s)	Phase (degrees)	VAF %
ag19	$-4.20e^{-6}$	$-1.61e^{-4}$	–0.76	5.64	7.21	98.01
fb13	$-1.97e^{-6}$	$-2.81e^{-4}$	–0.55	1.81	5.41	98.41
jn29	$1.75e^{-6}$	$-2.45e^{-4}$	–0.73	5.52	4.21	97.95
oc13	$-6.54e^{-6}$	$1.89e^{-4}$	–0.90	3.93	–0.60	98.12
mr16	$-2.27e^{-6}$	$-1.23e^{-4}$	–0.62	5.25	3.61	97.16
mean (18)	$-2.20e^{-6}$	$-1.88e^{-4}$	–0.69	2.92	3.57	N/A

x-y plot in normals was nearly linear with very small dc offsets (zero intercept; <8°/s). Note that this bias is not related in any way to the presence (or lack) of spontaneous nystagmus in the dark, as discussed earlier (Smith and Galiana 1991; Galiana et al. 1995).

The VOR of a representative normal subject is shown in Fig. 2A, with its associated x-y plot (Fig. 2B), after removal of a small 7.2° phase lead. In Fig. 2B, the fitted VOR characteristic curve (Eq. 1) is superimposed on the data points (bold line) and is clearly nearly linear. The parameters describing this particular normal VOR are provided in Table 1 (ag19, first row). (The gain and bias refer to the n and m coefficients in Eq. 1). Figure 3 superimposes the fitted VOR responses from five typical normal subjects, all estimated at the same peak velocity of 189°/s, at 1/6 Hz. The data fits for all our 18 normal subjects indicate a mean VOR gain of –0.68±0.16, a mean bias of 0.21±4.82°/s and a mean phase lead of 3.54±2.30°. At large peak head velocities, even the normal VOR can become non-linear, but remains symmetric; usually there is a decreasing sensitivity at higher speeds, with a few notable exceptions (example oc13 in Fig. 3 illustrates such a rare case). The presence of small biases in normal subjects (3–5°/s in Fig. 3) is understandable: any small asymmetry in a subject's bilateral sensory characteristics or central sensitivities would cause this, as simulated below.

Table 2 Sample vestibulo-ocular reflex characteristics with unilateral deficits

Subject	Cubic (q)	Quadr. (p)	Gain (n)	Bias (m, °/s)	Phase (degrees)	VAF %
nv10	$-2.90e^{-7}$	$9.94e^{-4}$	–0.55	7.23	14.43	97.01
mr31	$3.16e^{-6}$	$7.93e^{-4}$	–0.69	6.08	7.82	95.66
ap16	$-9.0e^{-7}$	$6.86e^{-4}$	–0.45	16.10	10.22	96.09
ja65	$2.80e^{-7}$	$4.11e^{-4}$	–0.46	6.52	10.22	98.67
mr02	$3.75e^{-6}$	$4.24e^{-4}$	–0.61	11.31	9.62	94.40
mean (50)	$1.24e^{-7}$	$-2.87e^{-5}$	–0.60	7.71	11.45	N/A

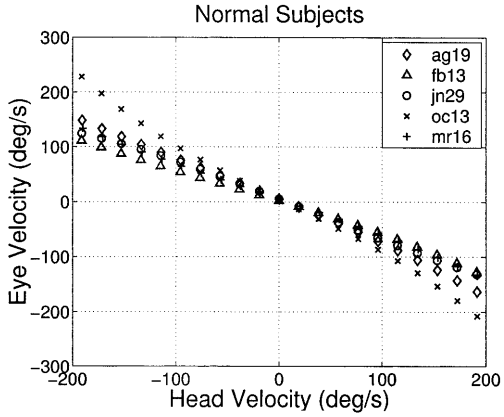

Fig. 3 X-Y plots of the polynomial fits to vestibulo-ocular reflex (*VOR*) data from five representative normal subjects (*symbols*)

Unilateral cases

In patients with a unilateral loss of peripheral vestibular function (determined by caloric tests), the phase shift of the VOR could be quite severe, even after long-term compensation (Table 2). Though a patient might no longer have had spontaneous nystagmus and might have felt close to normal, VOR phase leads could be four times the normal range (close to canal response phase). VOR gains were rarely larger than 75% of normal, and dc offsets were mildly elevated. The most striking change was the nature of the VOR eye-re-head characteristic. It was now clearly non-linear (requiring cubic fits) and asymmetric, with early saturation effects during faster rotations towards the side of the lesion.

An example is provided in Fig. 4A and B: a patient with a right vestibular deficit due to unilateral vestibular-nerve section. The right-side deficit appeared early as a *decreasing* sensitivity for rotations to the right above ~150°/s. The associated cubic fit for this VOR is superimposed on the x-y plot to better visualise its curvature. Other unilateral patients had even more severe deficits, displaying near saturation of the VOR gain for nearly all rotations towards the lesioned side. For ease of reference and in the interest of space, Fig. 5 provides the fitted VOR characteristics for only five of our unilateral patients, since the VOR with unilateral deficits has already been well described in the literature.

The data fits for all our 50 unilateral patients indicate a mean VOR gain (parameter n in Eq. 1) of –0.59±0.17, a mean bias of 7.67±6.61°/s and a mean phase lead of 11.51±4.41°. However, it must be noted that the gain figure is not a good description of behaviour in these non-linear patients. The parameter n is the linear term in the polynomial fit for the VOR characteristic and is best associated with the response during small head rotations (slope of x-y plot for small inputs). Hence, it is more appropriate to examine the full parametric description, as provided in Table 2. These relationships imply that, for unilateral patients, an incremental change in head velocity would cause a larger incremental change in eye velocity if added at low rather than high head speeds. Hence, VOR "gain" in patients is actually a dynamic measure, due to the non-linear behaviour. The typical "gain" figure (mean slope of VOR x-y plot) used in the clinic will, therefore, overestimate the performance of such patients during natural high-velocity head turns towards the side of the lesion.

Bilateral cases

In rotational tests of patients who had bilateral vestibular loss (determined by caloric tests), we expected little response due to a weak vestibular system. However, though there may have been little or no response during low head-velocity protocols (as expected), during higher-velocity protocols these patients usually demonstrated an *increasing* sensitivity in the response with increasing speed (example in Fig. 6). VOR characteristics appeared symmetric as for the normal subjects, but an unresponsive zone in the lower range of velocities in each protocol (dead-zone) seems obvious, especially in protocols with lower peak head velocities (see arrows in Fig. 6A). The percentage of a harmonic cycle spent in such a dead zone decreased as the maximum (or peak) input velocity increased; that is, VOR responses became smoother, albeit still non-linear during higher-speed protocols. As a result, cubic polynomials can produce reasonable fits to these VOR responses. Five typical bilateral cases are provided in Fig. 7 for comparison with the asymmetric characteristics of unilateral patients in Fig. 5.

The parameters from cubic fits of the VOR characteristics are provided for all 18 bilateral patients in Table 3. The linear gains obtained from these cubic fits were approximately 1/10 of the normal range (coefficient n in Eq. 1), with a mean of –0.09±0.19 for all 18 patients. The mean bias was –0.20±3.31°/s and the mean phase

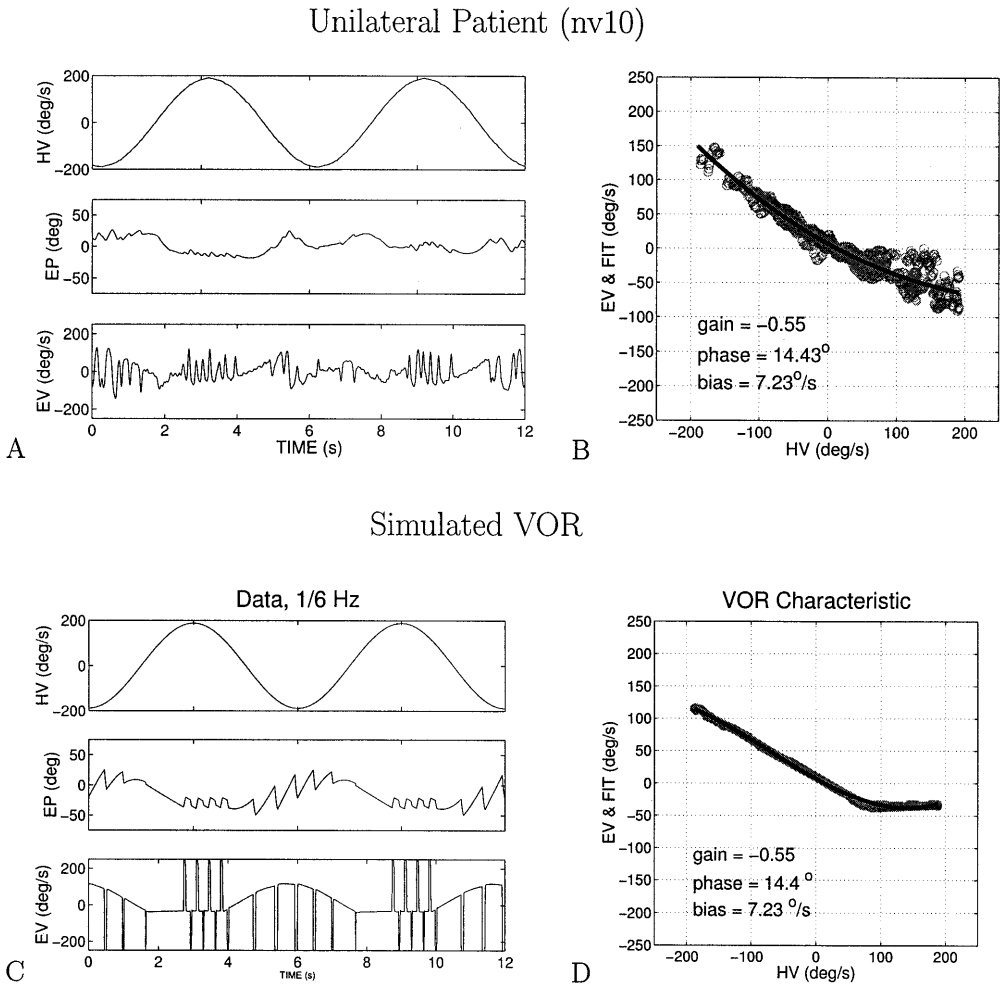

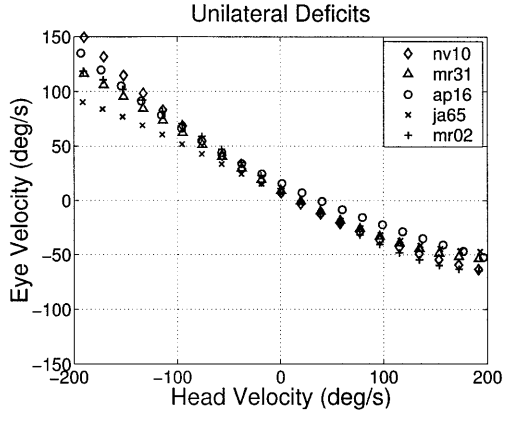

Fig. 4A–D Unilateral patient (nv10) with right vestibular nerve section. Same conventions as in Fig. 2

Fig. 5 X-Y plots of the fits to vestibulo-ocular-reflex (*VOR*) data from five representative unilaterally-deficient patients (*symbols*)

lead was 44.92±35.69°. The offsets are small because the response was small, but phase leads were approximately eight times the normal range; such large phase leads in bilateral peripheral patients were also reported by Hess et al. (1985).

This pattern of increasing VOR gain with concurrent head velocity appeared consistently in all bilateral patients, implying that in some cases the *incremental* VOR gain can be near normal, if perturbations were applied around high head velocities [e.g. slope of ~–0.6 in VOR x-y plot of patient fb12 at peak head velocities, but slope (VOR gain) of only –0.1 at low speeds, Fig. 7]. Thus, in contrast to unilateral patients, typical VOR "gain" figures (mean slope of VOR x-y plot) used in the clinic will now *underestimate* the performance of bilateral patients during natural high-velocity head turns.

Simulation of the VOR in normals and patients

Two types of non-linearities in the VOR have thus been seen. There is the more typical *decrease* in VOR gain (slope of x-y plot) with increasing head velocity, seen early on one side in unilateral patients or on both sides at high speeds in normals. Then, there is the surprising *increase* in VOR sensitivity in both directions as head speed increases in bilateral patients. The question here is whether these divergent behaviours require different hypotheses or whether both can be accommodated in a sin-

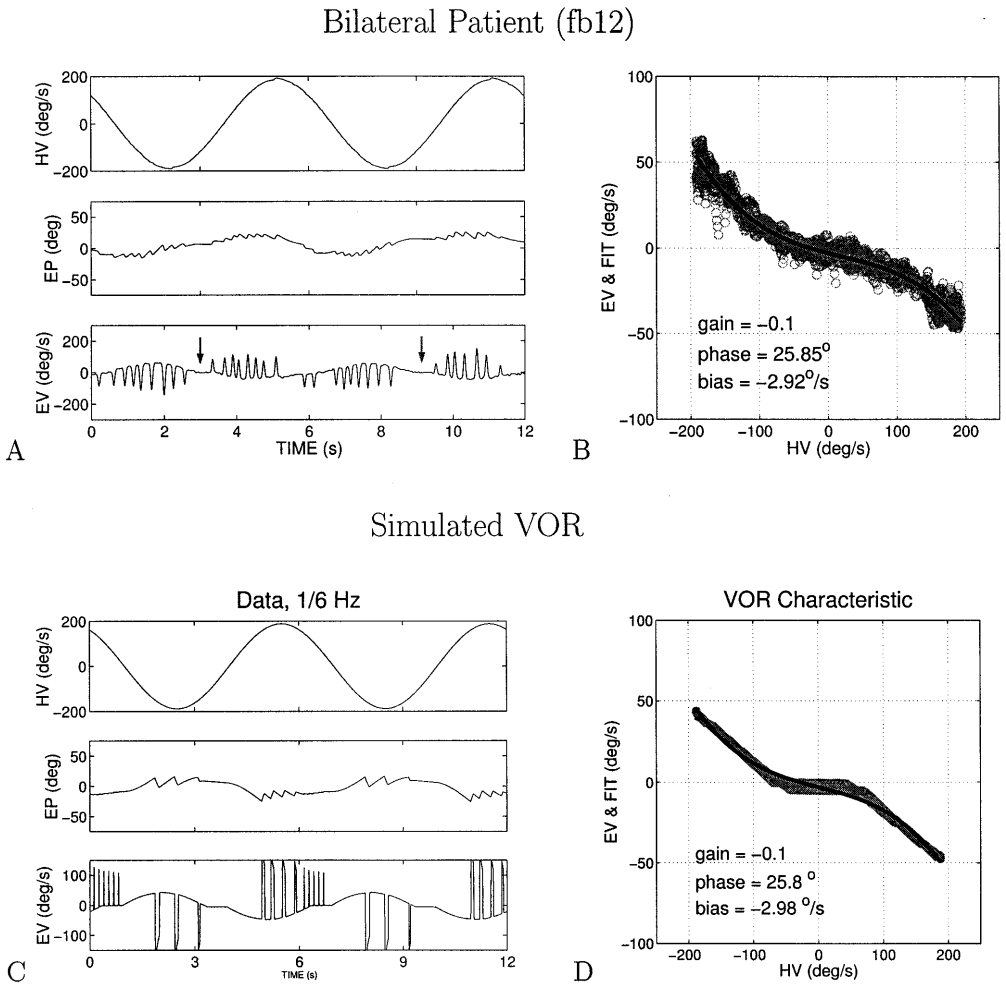

Fig. 6A–D Patient with bilateral deficits (fb12). Same conventions as in Fig. 2. *Arrows* in **A** point to apparent dead-zones in the vestibulo-ocular-reflex (*VOR*) traces

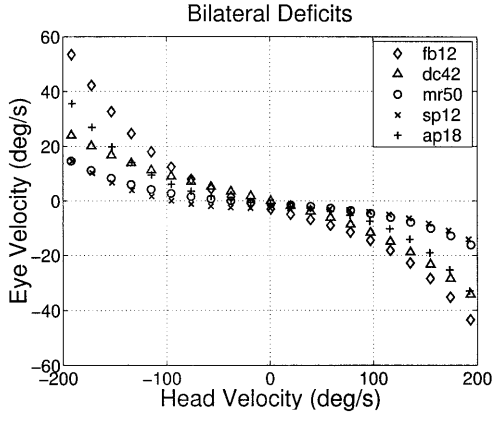

Fig. 7 X-Y plots of the fits to vestibulo-ocular-reflex (*VOR*) data from five representative bilaterally deficient subjects (*symbols*). Note the scale change on the vertical axis, compared with normals and unilateral-deficit patients (Figs. 3 and 5), because of low VOR gain

gle model with modified sensors. This was addressed by simulating the bilateral VOR model in the Appendix, with parameter sets selected to match examples from the three populations. Simple modification at the peripheral sensory stage, together with associated "compensatory" corrections centrally, seemed sufficient to reproduce behaviour.

Normal case

The parameters used in simulations of the normal VOR are consistent with our previous work (Galiana 1991; Smith and Galiana 1991). First, desired conditions are listed in the appendix (Table 4), which delimit preferred resting rates, time constants and sensitivities at different sites. The canal description assumes a simple linear sensitivity around a significant resting activity (line with slope k in Fig. 1A), such that primary responses are available for head rotation from 250°/s contralateral to 625°/s ipsilateral in the canal passband. The bilateral sensors are presumed symmetric with respect to each other, and each sensor projects onto one side of the bilateral model (see Figs. 12 and 13 in Appendix).

The time constants T_{vd} and T_{vc} (see Table 5 in Appendix) refer to the desired dynamics from the last bilateral stage, which implements gaze-holding integrators and is involved in both slow and fast phases. Additional parameters in the velocity storage stage transform the canal dynamics. Thus, the time constants of this velocity storage

Table 3 Vestibulo-ocular reflex characteristics in bilateral deficits (gain *n* not significantly different from zero, applicable at low head speeds)

Subject	Cubic (q)	Quadr. (p)	Gain (n)	Bias (m, °/s)	Phase (degrees)	VAF %
fb12	–4.01e^{-6}	2.27e^{-4}	–0.10	–2.92	25.85	96.42
dc42	–1.56e^{-6}	–1.34e^{-4}	–0.09	0.08	30.66	94.70
mr50	–1.50e^{-6}	1.10e^{-5}	–0.02	–1.00	27.66	63.78
sp12	–1.55e^{-6}	1.83e^{-4}	0.10	–5.58	114.83	34.72
ap18	–3.91e^{-6}	8.01e^{-5}	–0.03	–1.30	40.28	94.31
ap25	–9.37e^{-7}	4.69e^{-4}	–0.04	–4.17	54.11	62.29
fb09	3.10e^{-6}	2.03e^{-4}	0.15	–4.40	119.04	90.45
ja11	–6.03e^{-7}	9.18e^{-5}	0.01	–3.41	95.59	12.18
ja14	–4.20e^{-6}	3.71e^{-4}	–0.07	2.54	22.24	78.24
ja18	4.80e^{-7}	2.78e^{-5}	–0.05	–0.36	55.31	41.46
ja21	–1.41e^{-6}	5.91e^{-5}	–0.01	–1.21	21.64	57.33
ja26	9.54e^{-7}	8.98e^{-4}	–0.28	8.90	24.05	95.33
mr01	–6.93e^{-7}	–1.39e^{-4}	–0.05	0.86	30.06	64.43
mr07	–1.80e^{-8}	4.62e^{-5}	–0.01	–1.61	88.98	26.05
mr13	–5.39e^{-7}	–1.77e^{-4}	–0.004	1.53	10.82	19.93
sp17	4.06e^{-6}	–6.86^{e-5}	–0.38	0.22	4.81	78.62
nv17	–3.30e^{-7}	3.86e^{-5}	–0.05	–1.47	29.46	81.15
mr48	1.53e^{-6}	–2.61e^{-4}	–0.70	1.12	14.43	98.20
mean (18)	–6.18e^{-7}	1.07e^{-4}	–0.09	–0.68	44.99	N/A

stage (difference and common mode, T_{cd} and T_{cc} in Table 5) will replace the canal time constant in the VOR behavioural response, provided that the "integrator" time constant (gaze holding) in the last stage is large. In the normal case considered here, the *apparent* global VOR time constant (as per phase lead re head velocity) will change from 4 s at canal levels to over 16 s at the behavioural level.

Figure 2C, D is a simulation of the VOR in a normal subject, during a peak rotation velocity of 189°/s. The parameters were selected to represent the subject above in the same figure. Fast phases are more likely as head velocity increases, and their frequency is slightly higher to the left. This is associated with the small dc bias on the resulting model VOR characteristic (Fig. 2D), also observed in this subject. The VOR characteristic appears nearly linear, even though central resting rates and sensitivities would not have allowed such ideal behaviour in a sustained slow-phase mode response (pure VOR compensatory mode). Two mechanisms contribute together to reflex linearity at central stages in this model: the bilateral nature of the premotor circuits in the VOR (Smith and Galiana 1991) and the resetting action of fast phases on premotor cells (Galiana 1991). The result is a normal VOR characteristic compatible with central and behavioural data. We can thus move on to lesion cases.

Unilateral case

In a unilateral vestibular lesion, there is a presumed reduction of the primary vestibular response on the side of the experimental VOR (X-Y) plot, corresponding to rotation towards the lesion side (during rightward head velocities for a right lesion). In general, to represent a unilateral deficit, the lesioned-canal sensitivity curve can be shifted downwards (a reduction in the canal resting rate) and towards the lesion side (a reduction in sensitivity); or, in the case of a total loss, it is driven to zero (Fig. 1B).

To preserve central properties and match observed behaviour, the two sides in the *central* stages may now have different (endogenous) resting rates and sensitivities to reflect the consequences of compensation that rebalances central background activity at vestibular-nuclei (VN) and premotor levels (R_v and R_e). The remaining model parameters are then selected to fit the patient's VOR gain and phase characteristics, through appropriate time constants (see Appendix). For example, if gaze holding was intact, then the parameters in the velocity storage stage would be selected to imbed the observed VOR phase, and the second stage set to provide the appropriate gaze-holding time constant (near 15 s). If gaze holding was deficient, then after providing the appropriate time constant in the second bilateral stage, the required time constant in the velocity storage stage had to be set smaller than expected from the observed VOR phase, due to the beneficial effects of nystagmus on the global VOR phase. The adjustments used here centrally are compatible with observations after unilateral vestibular loss: realignment of resting activity and improvement of VOR gain require changes in the sensitivity of premotor cells in the VN to both commissural and primary afferent signals (Newlands and Perachio 1990; Chan et al. 1999; Yamanaka et al. 2000; see also reviews by Dieringer 1995; Curthoys and Halmagyi 1995). Such synaptic changes theoretically can cause associated changes in the dynamics of central circuits, particularly associated with asymmetries in central *modulations*, despite appropriate ocular responses (Galiana 1985).

Here we present simulation results for the case in Fig. 4, a patient who underwent a unilateral vestibular nerve section. Thus, the remaining canal in the model preserved a normal linear function, while the other was forced to zero (Fig. 1B); what is more surprising is that it

was also necessary to postulate a reduction in resting rate in the remaining healthy canal, so that its linear functional range is now modified (range of operation is from 798°/s ipsilateral to 78°/s contralateral; see Fig. 1B). Possible mechanisms for this postulate are proposed in the Discussion.

The observed VOR phase lead in this patient is presumed to be a reflection of the interaction between primary dynamics and the "velocity storage" stage, since gaze holding was normal (T_{vd} was large, see Methods). In the model here, this required decreases in commissural excitation in the first stage, together with increased (possibly asymmetric) commissural inhibition in the vestibular-nuclei/prepositus hypoglossi (VN-PH) (premotor) stage. The full parameter set for this unilateral simulation is provided in the Appendix (Tables 4, 5, 6, 7). Figure 4C and D is a simulation of this unilateral patient at a peak rotation velocity of 189°/s. It exhibits the characteristic asymmetry in the number of fast phases in each direction, due to reproduction of the small but significant dc bias seen on the experimental VOR characteristic (Fig. 4B,). The linear range of the VOR in this unilateral patient simulation is much smaller than normal (<100°/s ipsi-lesion head rotation), but is compatible in this case with that of the remaining canal during contra rotation (~80°/s, Fig. 1B). The EV during ipsi-lesion rotation now saturates around –38°/s. However, the non-linear VOR characteristic can also be dominated by central, not peripheral, properties (see Discussion).

We found that the shape of simulated VOR characteristics in this model could well match those of any unilateral patients and stay compatible with the known etiology. For example, in order to duplicate the VOR characteristics of patients with non-specific unilateral disease (e.g. Meniere's disease), reproduction of behaviour required that the deficient canal be represented by a more non-linear (sigmoidal) characteristic as per the first option above, rather than simply forcing its response to zero (nerve-section case).

Bilateral case

To represent bilateral lesions, the canal resting rate, *Rc*, was reduced to zero and a curved characteristic for the canal sensitivity was shifted outwards on both sides to implement a dead-zone (Fig. 1C). Such non-linear sensory properties were sufficient to reproduce the data, without changing the dynamics of the torsion-pendulum effect (remains at 4 s). As a result, the VOR circuit is again symmetric, but the reflex must now overcome a large threshold and there is a global decrease in primary sensitivity. Internal activities in the central stages of the model (R_2 and R_3) were again readjusted to keep effective central resting rates near their normal levels, presumably achieved in the patient during the compensation process. This would be consistent with the known near-recovery of central resting activities in unilateral lesions, but, to our knowledge, no one has recorded in the vestibular nuclei of alert animals after otoxicity (acute or recovered). To reproduce the abnormally large phase leads (worse than expected from canal response), the commissural pathways in the first velocity-storage stage had to reverse from net mutual excitation to net mutual inhibition. To compensate for lower velocity-storage (VS) resting rates and low sensory sensitivity, a decrease in mutual inhibition in the premotor stage and a generalised increase in sensitivity to afferent vestibular signals were required.

Figure 6C and D summarise the effects of these sensory changes in the model, with parameters tuned to represent the patient in Fig. 6A and B. At the lowest velocity, the canals are very close to cut-off so that the eye response is near zero while, at the highest rotation velocity, one or the other canal responds well. The result is an apparent improvement in VOR gain for protocols with larger peak velocities, the increasing sensitivity observed experimentally (Fig. 6B). In fact, the instantaneous gain of the VOR (slope of x-y curve at a given head velocity) can even reach normal levels, depending on the severity of the attenuation in sensory transduction and/or quality of central compensation. However, *mean* gain is still low compared with normal subjects, and phase leads are large (Table 3). The proposed canal characteristic could be due to thresholds for the activation of neural transduction in each canal and velocity-dependent recruitment of damaged haircells, which is consistent with the nature of most causes of bilateral lesions, such as ototoxicity or presumed peripheral cell loss secondary to microangiopathy (see Discussion).

Discussion

This study combined experimental data and simulations to explore the underlying causes of non-linearities in the human VOR in patients with unilateral or bilateral deficits of peripheral function. Simple changes in primary sensory characteristics were sufficient to explain the diverse VOR non-linearities of both unilateral and bilateral losses: asymmetries with *decreasing* VOR gain at high speeds in unilateral patients versus symmetric characteristics in bilateral patients with *increasing* VOR gain at higher speeds. Central non-linearities representing limits on cell responses play a crucial role, so that behaviourally observed VOR characteristics will depend on the protocol rotation speeds, rotation frequencies and the nystagmus pattern itself. In the presence of sensory deficits, compensatory changes in central endogenous activities (model internal biases) are required to restore functional ranges in central circuits and reduce biases causing spontaneous nystagmus. The main postulated sites of compensatory changes are summarised in Fig. 8. However, to maintain desired resting rates and central sensitivities to head rotation (see Table 4 in Appendix), minor parametric changes are in fact required at multiple sites in this distributed processor (see Table 5 in Appendix).

This simulation study provides an alternative formulation for the processing stages proposed by Lasker et al.

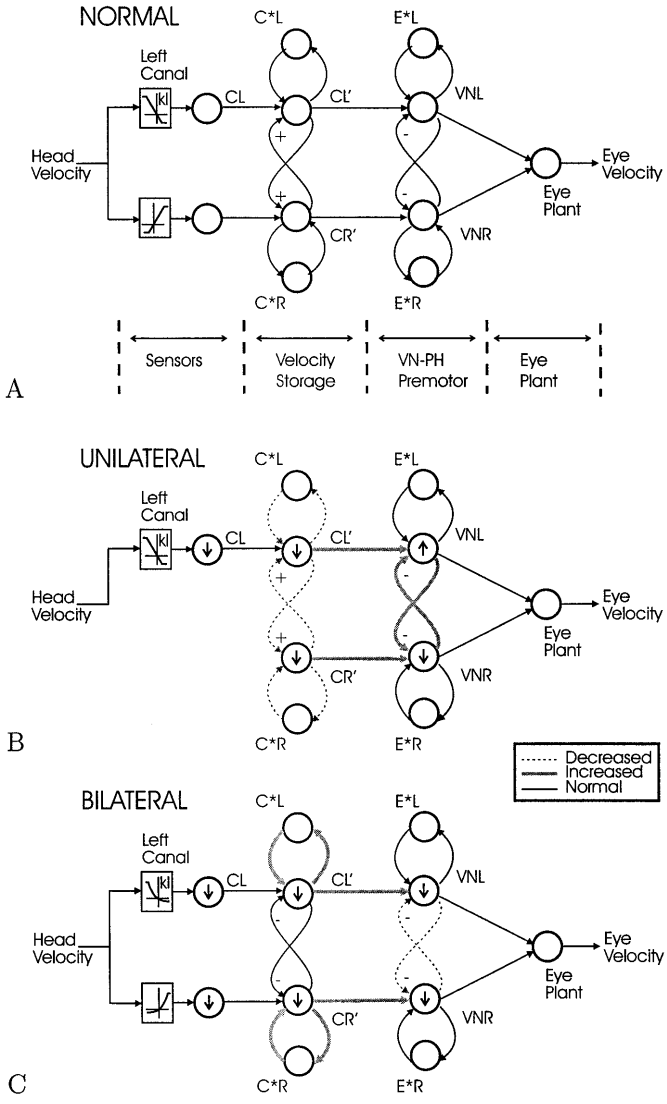

Fig. 8A–C Schematic diagrams of model stages detailed in the appendix. *Inserts* show line conventions for *significant* changes in projection strengths, and *imbedded arrows in circles* denote changes up or down from normal in each nucleus resting activity. **A** Balanced conditions in the normal case. **B** Unilateral right lesion associated with decreased commissural excitation in velocity-storage (VS) stage to achieve correct phase and increased mutual inhibition in vestibular-nuclei/prepositus hypoglossi (VN-PH) premotor stage. **C** Bilateral deficit associated now with net commissural inhibition in first stage to achieve large phase lead, and decreased mutual inhibition in premotor stage to partially improve the premotor resting rate. For definitions of abbreviations, see Fig. 12 in Appendix

(1999, 2000) in the monkey VOR. These authors explained the significant non-linearities of the VOR after compensation for unilateral labyrinthectomy, by proposing a greater reliance on irregular (non-linear) rather than regular (linear) primary afferents at central levels: that is, the central VOR was proposed to consist of two parallel pathways, one linear and the other non-linear on each side of the brainstem, with modifiable recruitment. This may be very difficult to test experimentally. Instead, it is proposed here that simple changes in the sensory characteristics (static non-linearity) due to disease or lesions are sufficient to explain the data in both unilateral and bilateral cases, because they are necessarily associated with central parametric changes to provide compensation: here, cell firing-rate limitations at all stages, and the need for bilateral "balance", will always result in new VOR dynamics and non-linearities secondary to sensory deficits. Specific changes in primary recruitment patterns may exist, but are not required. Several issues related to assumptions made in the model simulations will now be discussed. They point to some key experiments to verify model predictions for the compensation process after vestibular lesions and to several implications for the clinical evaluation of functional recovery in the vestibular patient.

Are healthy primary regular afferents linear or non-linear?

The first processing stage in any VOR model requires an adequate representation of activity on primary vestibular fibres. There is a current controversy on whether we should bother with non-linear descriptions of canal function, especially during natural (high-frequency) head movements. We will focus on regular vestibular afferents, since they are known to play the dominant role in the normal rotational VOR (Minor and Goldberg 1991; Chen-Huang et al. 1997). In their early seminal work in the squirrel monkey, Goldberg and Fernandez (1971) reported significant asymmetries in the responses of regular afferents to ipsilateral versus contralateral steps of acceleration. Figure 9A well reproduces the responses of a particular regular fibre provided in their paper (Fig. 15 in Goldberg and Fernandez 1971), using a simple non-linear (asymmetric) model of canal function (ipsi-/contralateral sensitivity to *acceleration*: 2.2 vs. 1.62 sp/s/°/s^2; ipsi-/contralateral time constant: 6.96 vs. 4.01 s). The non-linear nature of similar regular afferents is again strongly supported in more recent work (Brichta and Goldberg 2000), where the turtle regular afferents also exhibit a form of decreasing sensitivity with increased head velocity (as in the sigmoidal curves of Fig. 1).

How can this be reconciled with the reported linear behaviour of regular afferents in chinchilla during high-frequency sinusoidal head rotations above 0.5 Hz (Hullar and Minor 1999)? One could call on species differences. However, the answer could be that interactions between transduction dynamics and static non-linearities can change the *apparent* sensory characteristics, depending on the stimulus properties (head-velocity frequency, amplitude,...). For example, in Fig. 9B, C, the identical non-linear sensor model used in Fig. 9A is now subjected to 1/6-Hz head rotations, the conditions used in our protocols. Clearly, the sensor now appears to behave in a very linear fashion (Fig. 9C), with an apparent velocity sensitivity of ~0.5 sp/s/°/s and an effective time constant of ~5 s. Hence, a non-linear sensor can be adequately repre-

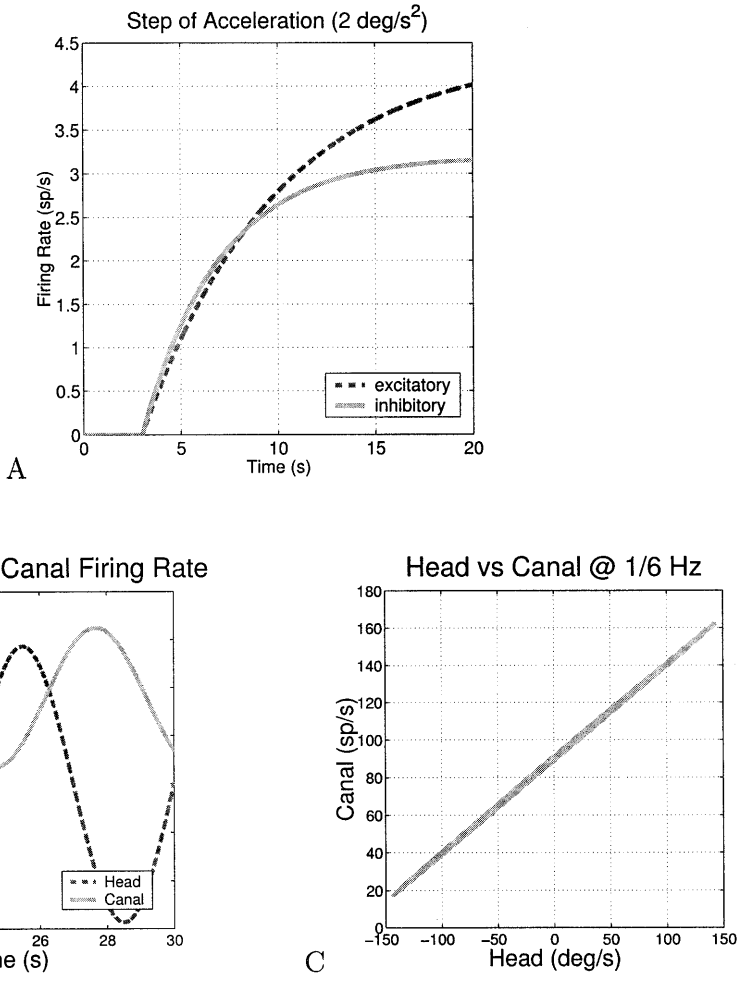

Fig. 9A–C Effects of sensory non-linearities on canal nerve responses. **A** Results from a Simulink model reproducing asymmetric data of Goldberg and Fernandez (1971) during steps of acceleration (see Discussion). **B** Responses from the same model to 1/6-Hz head rotation at peak speeds of 150°/s. **C** X-Y plot of data in **B**, with apparent linear characteristics at 1/6 Hz

sented by a linear process (subject to cut-off or saturation) in this particular case, or at the frequencies used by Hullar and Minor (1999). It is the basis for assuming straight-line characteristics in our canal models here, so long as the sensor is healthy and the protocol conditions allow it. Changing the protocols would normally require re-examining assumptions of linearity, especially at low frequencies. In general, it would be preferable to imbed the true non-linear behaviour in all cases, even though apparent linear function may sometimes be observed.

However, this issue of sensor "linearity" is not critical to reproducing observed clinical data after total *unilateral* loss: a linear form of the remaining vestibular function is quite sufficient, so that the main non-linear properties of the VOR observed behaviourally could simply be due to limitations in the remaining peripheral sensor's range of operation and/or the asymmetric properties of the brainstem after compensation. This is not the case for more labile unilateral deficits or for bilateral lesions due to ototoxicity (see below): in these cases, reproduction of non-linear VOR characteristics did require assuming more non-linear (sigmoidal) descriptions of canal function – a verifiable model prediction (see below).

VOR after unilateral lesions – peripheral or central non-linearity?

A wide variety of non-linear VOR forms could be represented by simple changes in the global *static* non-linearity of the lesioned sensor characteristics (see also "'Velocity storage' and VOR phase lead", below). The time constant of the vestibular torsion-pendulum model was always presumed unchanged since it reflects the mechanical properties of the cupula (see also "Bilateral patients", below). Similarly, additional *new* central non-linearities in the brainstem processes were not required, only parametric changes to realign bilateral resting activity (biases) and to achieve the observed VOR phase and gain. All types of responses could be duplicated in one model, by making changes compatible with the known lesions considered here (see also section "'Velocity storage' and VOR phase lead", below).

The VOR model simulations of a unilateral loss patient (Fig. 4) were achieved with parameter sets tuned for our 1/6-Hz protocols. In order to test the reliability of our hypothesis, this model was also used to generate predicted responses to harmonic rotations (Fig. 10) or to steps of head velocity (Fig. 11), always with the *same* parameter set as in Fig. 4. The simulation result in

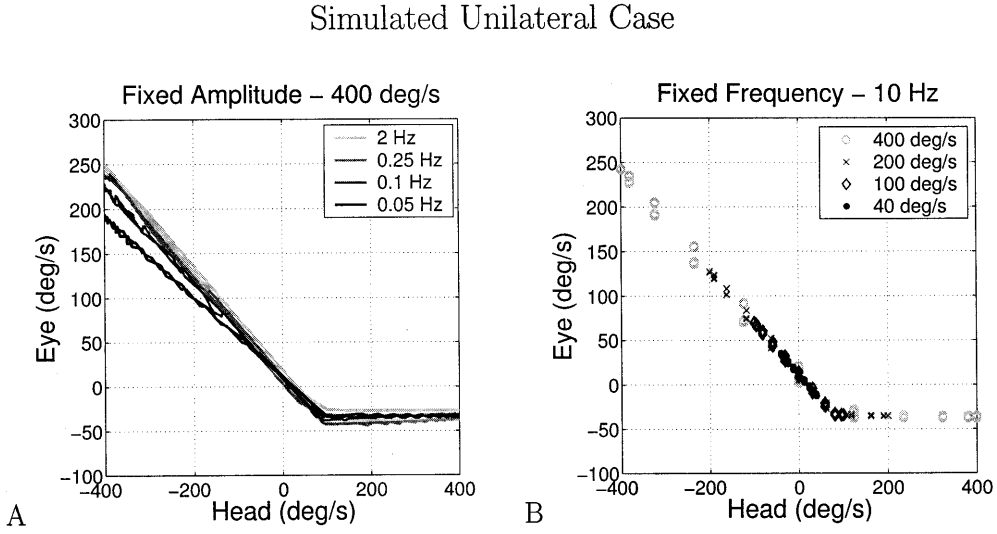

Fig. 10A, B Harmonic simulations of vestibulo-ocular reflex (*VOR*) model used in Fig. 4 (right lesion). **A** Different rotation frequencies and a fixed peak head velocity cause changes in observed VOR gain; note ipsi-contra peak response asymmetry increases with frequency. **B** With a linear sensor in its functional range, different peak head velocities at 10 Hz do not modify the resulting VOR characteristics

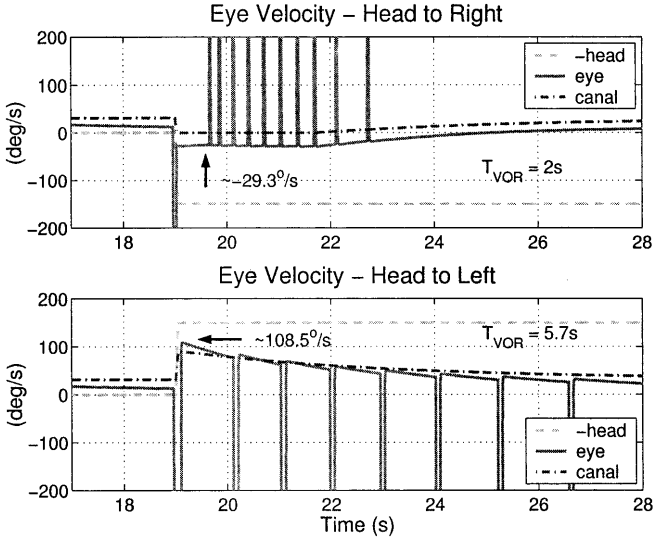

Fig. 11 Simulation of vestibulo-ocular reflex (*VOR*) model used in Fig. 4, during steps of ipsi-lesion vs. contra-lesion head rotation at 150°/s. Note apparent variable VOR decay rates and different saturation level when compared with 1/6-Hz simulation in Fig. 4 (head velocity trace is reversed)

Fig. 11 reproduces the types of VOR responses observed experimentally in compensated, unilateral mammals: asymmetric step responses, saturation during rotations ipsilateral to the lesion and differences in the apparent decay time constants with rotation direction (after leaving saturation level, Fig. 11). The model's non-linear behaviour is also qualitatively similar to that reported previously in other experimental reports (Broussard et al. 1999; Lasker et al. 2000): for example, apparent changes in the severity of VOR asymmetry as the stimulus frequency changes (Fig. 10A, slopes at peak ipsi- and contra-lesion rotation) and an apparently more robust contra-lesion sensitivity for high-frequency 10-Hz rotation at different speeds (Fig. 10B).

In the simulation at 10 Hz (Fig. 10B), the non-linearity in fact now remains relatively stable with stimulus amplitude, despite a "gain" variability with input *frequency*. Reported changes in VOR contra-lesion sensitivity at high frequencies are much smaller than at low frequencies and do not appear statistically very significant above a few Hz (Minor et al. 1999; Lasker et al. 2000). Our current model does not produce variable gains at *high* frequencies unless sensor or central cells have input-dependent non-linearities themselves (curved sensitivities). This is to be developed in the future. With non-linear (curved) VOR behavioural characteristics (as implied in Fig. 4B), a global VOR characteristic could be an appropriate *single* description of the reflex at a given frequency; however, forcing sine-wave fits for half-cycles (as in Broussard et al. 1999; Lasker et al. 1999, 2000; Minor et al. 1999) could still produce *estimated* VOR gains that vary both with input amplitude and direction, depending on the form of the non-linearity. This half-cycle approach essentially fits an optimal straight line through a non-linearity for each input amplitude: with a VOR curve as in Fig. 4B, the resulting fit can have higher slopes for higher inputs when the non-linearity is "bowl-shaped"; on the other hand, if the non-linearity in the test conditions appears to be "saturating", then the estimated gain (line slope for sine fit) would decrease with input amplitude. Results are then labile and depend on which part of a larger non-linearity is being exercised. A non-linear system can be very difficult to interpret in a coherent way if analyses are restricted to linear tools.

Note that the remaining canal in the cases above was assumed linear, with a modified range of operation. This caused sensor cut-off for the first 1.5 s of the step response during ipsi-lesion 150°/s rotation (see dotted lines in Fig. 9, top panel). The ipsi-lesional response saturated at ~–30°/s, which is less than the saturation level observed during 1/6-Hz simulations (Fig. 4D). Again, the observed non-linearities in this simulated VOR reflect

the combined effects of primary non-linearities, primary dynamics (lower gain at lower frequencies extending the operating range) and possibly *asymmetric* central modulations about a balanced, and reduced, resting activity (Galiana 1985). (Remember that the *initial* segments of a VOR step response actually represent a *high-frequency* test.) Saturations in the VOR during various protocols, therefore, need *not* represent an unmasking of the non-linear limits in the single remaining vestibular sensor, but can also reflect rectification (cell cut-off) in some premotor centres.

Finally, a non-linear sensory characteristic (peripheral) was implied by the model-fit requirements in many non-specific patients. This is a prediction that remains to be verified in animal models. More to the point, much is known of the changes in vestibular nuclei activity after unilateral vestibular loss (see reviews in Curthoys and Halmagyi 1995; Yamanaka et al. 2000), but there is currently no information to support the standard assumption of normal characteristics in the remaining vestibular sensors (primary activity) after such losses. Perhaps the compensation process is assisted by the vestibular efference system, which would acutely carry bilaterally unbalanced activity and could at least temporarily alter the primary dynamics and/or resting activity (Brichta and Goldberg 2000; Marlinski et al. 2000). The same question would be relevant for animal protocols involving canal plugging: can the primary system dynamics or non-linearity be altered by now bilaterally asymmetric modulations at central levels, despite normal resting activity?

Bilateral patients

In the bilateral patients, reproduction of VOR non-linearities relied on one key assumption: deficits in the bilateral sensors including a threshold (dead-zone), and sensitivities much lower than normal. No change of canal *dynamics* was required. These represent predictions of the sensory process in man after otoxicity or cell death due to suspected microangiopathy (our patients). However, we can infer that these are reasonable results in relation to reported observations in the pigeon (Li and Correia 1998). After exposure to toxic doses of streptomycin, canal primary-afferent activity in the pigeon was monitored throughout the recovery process (up to 150 days post-injection): canal *dynamics* never changed significantly from the control condition. In the initial phase, primary activity had greatly reduced resting rates and much lower sensitivities to a wide range of stimuli. In the pigeon, 150 days seemed sufficient to restore normal sensitivities, but resting rates remained at ~50% of normal. Thus, given our data and model predictions here, it would seem that man never fully recovers from otoxicity and that the primary fibre responses resemble those observed acutely in the pigeon.

Another model prediction for many bilateral patients was a sensory process with *increasing* sensitivity at higher rotation speeds. Increasing sensitivity with increasing stimulus amplitude is seen on normal primary activity at *low* head speeds (see Introduction and the section “Are healthy primary regular afferents linear or non-linear?”, above); hence, it seems reasonable that this non-linearity may become more important when operating at low gain with modified vestibular morphology (the lower end of the sigmoidal curve in Fig. 1). This conjecture seems consistent with pigeon data (see above), but we are not aware of experimental data on primary vestibular afferents in mammals or primates after otoxicity. Hence, it remains to be verified whether the observed VOR non-linearities are indeed sensorial in our bilateral patients.

The model predicts, at least in our pool of bilateral patients, that normal levels of VOR response might appear at high rotation speeds, if tested with head perturbations applied around a high speed bias [e.g. slope of ~–0.6 in VOR x-y plot of patient fb12, at peak head velocities but slope (VOR gain) of only –0.1 at low speeds, Fig. 7]. Thus, as in the unilateral patients, clinical evaluation of VOR integrity is keenly dependent on the selected head-rotation protocol.

“Velocity storage” and VOR phase lead

In most patients, the final compensatory result was always associated with net deficits in the measured VOR phase, causing abnormally large phase leads at the test frequency. Thus, it would seem that central loop recruitment is reduced in the post-lesion state, since feedback is an accepted mechanism for “storage” action. Here, we simply postulated a parametric change in a “velocity storage” model stage. Equivalently, a model where cell and loop recruitment in the bilateral stages depended on current set-point would achieve the same result, since bilateral resting rates at VN levels have been shown to be decreased in animals after compensation for peripheral vestibular lesions. Thus, the parametric changes at the central level are interpreted here to be *secondary* to the assumed change in sensory afferent signals: because of the non-linear and highly interconnected circuits in the brainstem, modifying sensory inputs would naturally change the functional dynamics of the downstream premotor circuits.

The present study relied on a two-stage representation of VOR processing after the sensors: velocity storage and pre-motor “neural integration”, as often postulated in the literature (Raphan et al. 1977). The same effect could be achieved with a single bilateral stage, where two imbedded feedback loops interact to improve canal dynamics and cancel eye plant dynamics simultaneously. Available neurophysiology and anatomy cannot yet specify which type of model topology is most appropriate. However, this is not significant from the point of view of this study. Here, the intent was to demonstrate that *peripheral* sensor modifications could dominate in reproducing observed VOR characteristics

in normals and selected patients, if one also takes into account non-linearities in central circuits associated with compensation and the dynamic effects of nystagmus on the reflex.

This modelling exercise attempted to duplicate experimental data based on an understanding of the equations representing the simulated model behaviour. In the future, it is planned to develop automated identification procedures that would fit data to alternate central topologies without subjective biases.

Acknowledgements This work was supported by an operating grant from the Medical Research Council (MRC, Canada). We also thank J. Goldberg for his helpful comments on the characteristics of vestibular nerve responses.

Simulink models of the VOR with selected parameter sets

The two figures included here (Figs. 12 and 13) describe the implementation of the VOR in the Simulink (Matlab) environment, for those who wish to duplicate or test model properties. Figure 12 is a bilateral realisation of the slow phase and includes sensory, velocity storage, central integration and motor stages. At all appropriate levels, central background activity (resting rates) and neural saturations are also represented.

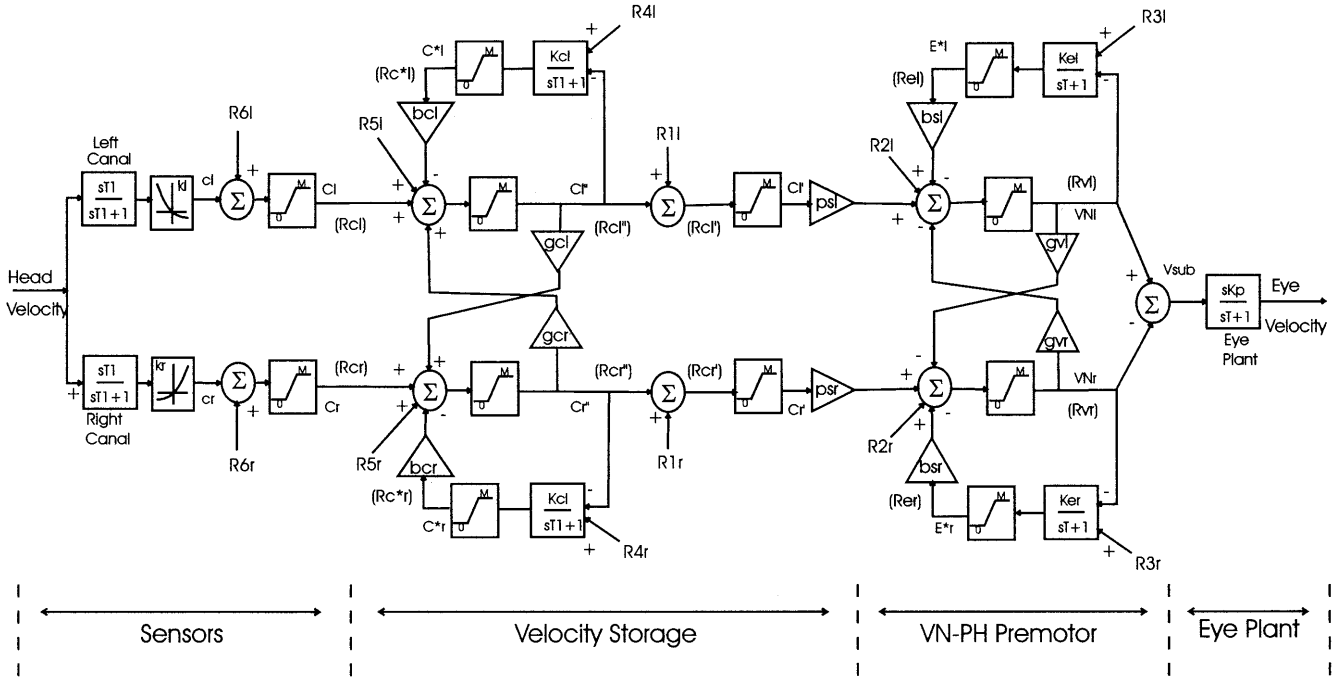

Fig. 12 Schematic of the vestibulo-ocular reflex (VOR) model during slow phases. Transfer functions are shown for: canal modulation (*cr, cl*), eye plant and internal models generating efference copies of right and left ocular/canal responses (*E*r, E*l, C*r* and *C*l*). Canal non-linearity defined in Fig. 1. *Cr/Cl* Right and left canal firing rates, combining modulations with resting rate *Rc*; *VNr/VNl* premotor vestibular nuclei firing rates; *gv/gc* commissural (cross-midline) pathway gains in two stages; *bc/bs* ipsilateral loop gains in two stages, which control time constants together with commissural gains. Endogenous or external biases (e.g. *R1–R6*, right and left) are used to reach desired resting rates in different sites when head velocity is zero. *VN-PH* Vestibular-nuclei/prepositus hypoglossi. For other definitions, see text and Table 4

Table 4 Model characteristics forced constant in all cases (refer to Fig. 12)

Site	Description	Parameter	
Sensors	Canal time constant	T1	4.1
Velocity storage	Canal "model" gain	Kcr	0.5
		Kcl	0.5
	Canal "model" resting rate (sp/s)	Rc*r	60
		Rc*l	60
VN-PH premotor	Eye model gain	Ker	0.5
		Kel	0.5
	Eye model resting rate in PH (sp/s)	Rer	90
		Rel	90
Eye plant	Eye plant (and model) time constant	T	0.3
	Eye plant gain	Kp	0.55
Saturation	Maximum firing rate (sp/s)	M	350

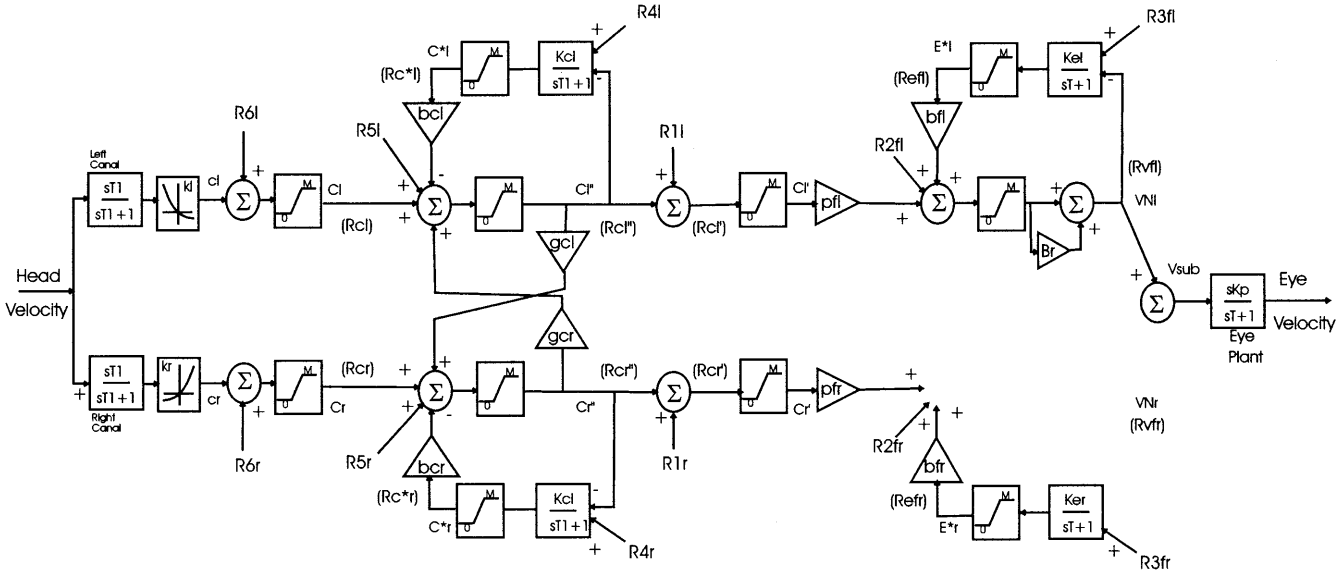

Fig. 13 Schematic of the vestibulo-ocular reflex (VOR) during fast phases to the right (mirror image for leftward fast phases). The right vestibular-nuclei (VN) is driven into cutoff by right bursters, disabling commissural coupling in the second (premotor) stage. [Parameters in the first velocity-storage (VS) stage same as in slow phase.] The premotor stage (with burst cells *Br*, *Bl*) uses new parameters to replicate effects of switching and enable fast phase dynamics (see Tables 4 through 7). Conventions as in Fig. 12

Table 5 Slow-phase model parameters that vary with type of deficit (* indicates significant changes from normal; *computed items* refer to desired values achieved with the associated parameters)

Site	Description		Cases			
			Name	Normal	Unilateral	Bilateral
Sensor	Canal afferent resting rate (sp/s) (*computed*)		Rcr	100	0*	3.33*
			Rcl	100	62.5*	3.33*
	Canal bias (sp/s)		R6r	100	0*	–2.5*
			R6l	100	31*	–2.5*
	Linear approximation of primary neuron gain	Excitatory	ke	0.4	0.4	0.146*
		Inhibitory	ki	0.4	0.4	0.096*
	Curved approximation of primary neuron gain (Eq. 3)	Quadratic term	a	0	0	2.09e^{-5}*
		Linear term	b	0.4	0.4	0.092*
Velocity storage	VOR time constants *(computed from data)*	Diff. mode	Tcd	7.42	4.23*	1.37*
		Common mode	Tcc	7.49	4.23*	1.38*
	Slow phase ipsi-loop gain		bcr	0.9	0.06*	–3.95*
			bcl	0.9	0.06*	–3.95*
	Commissural gains		gcr	0.005	0.001*	–0.005*
			gcl	0.005	0.001*	–0.005*
	Output bias (sp/s)		R1r	0	–80*	–90*
			R1l	0	20*	–90*
	Canal model filter bias (sp/s)		R4r	201.45	125*	–237*
			R4l	201.45	124*	–237*
	Input (endogenous) bias (sp/s)		R5r	50.05	150*	153*
			R5l	50.05	92*	153*
VN-PH premotor	Integrator time constants, *computed*	Difference mode	Tvd	13	6*	8*
		Common mode	Tvc	1.5	1.0	1.7
	VN gain re canal (*computed*)		Sv	1.7	2.6*	7.0*
	Slow phase input gain		psr	0.48	0.69*	2.03*
			psl	0.48	0.69*	2.03*
	Slow phase ipsi-loop gain		bsr	1.76	1.63	1.78
			bsl	1.76	1.63	1.78
	Commissural gains		gvr	0.10	0.16*	0.08*
			gvl	0.10	0.16*	0.08*
	Input bias (sp/s)		R2r	155.73	186.5*	212.5*
			R2l	169.32	130.7*	204.1*
	Eye model filter bias (sp/s)		R3r	221.37	216*	229*
			R3 l	233.72	205*	221*

Table 6 Fast-phase model parameters forced constant in all cases (this only affects the vestibular-nuclei/prepositus-hypoglossi (*VN-PH*) stage, previous stages remain at same settings throughout nystagmus)

Site	Description	Parameter	
VN-PH premotor	Eye model resting rate (sp/s) (*computed*)	Refr	90
		Refl	90
	Burst cells gain	Br	2.0
		Bl	2.0
	Time constant *(computed)*	Tf (s)	0.05
	Input "vestibular" gain	pfr	–1.2
		pfl	–1.2
	Ipsi loop gain	bfr	3.33
		bfl	3.33

Table 7 Fast-phase model parameters which vary with type of deficit (refer to Fig. 13; note asymmetries in saccade thresholds in unilateral case)

Site	Description	Name	Cases		
			Normal	Unilateral	Bilateral
VN-PH Premotor	Input bias (sp/s)	R2fr	–166	–213	–284
		R2fl	–162	–216	–286
	Eye model filter bias (sp/s)	R3fr	221	213	229
		R3fl	234	205	221
Switching	Fast-phase ON threshold (sp/s)	Onthresr	24	78	47
		Onthresl	24	2	40
	Fast phase OFF threshold (sp/s)	offthresr	150	56	2
		offthresl	150	25	2

The schematic during fast phases is altered by the effect of central burst cells, so that a representative model for rightward fast phases is provided in Fig. 13. Simple mirror symmetry would describe the model during leftward fast phases. Note that switching between slow and fast phases involved switching the appropriate parameter values into pathways: the same dynamic elements (integrators) were shared by both modes.

The parameter sets used in the three representative simulations (see Results) are described in Tables 4, 5, 6 and 7. Parameters refer to elements in models of Fig. 12 and 13. T_{cd} and T_{cc} represent the time constants of the "velocity-storage" stage, used to match VOR phase. Similarly, T_{vd} and T_{vc} represent time constants computed for the vestibular-nuclei/Prepositus hypoglossi (VN-PH) stage and implement the oculomotor integrator properties. The integrator (T_{vc}, T_{vd}), velocity storage (T_{cc}, T_{cd}) and fast phase (T_f) time constants can be computed from Eq. A-1, when matches to the patient data are related to model parameters.

$$
\begin{aligned}
T_{vc} &= T\cdot(1+gv)/(1-Ke\cdot bs+gv)\\
T_{vd} &= T\cdot(1-gv)/(1-Ke\cdot bs-gv)\\
T_{cc} &= T\cdot(1+gc)/(1-Kc\cdot bc+gc)\\
T_{cd} &= T\cdot(1-gc)/(1-Kc\cdot bc-gc)\\
T_f &= T/(1+Ke\cdot bf\cdot(1+B))=50\text{ ms}
\end{aligned}
\qquad \text{(A)}
$$

References

Baker R, Evinger C, McCrea RA (1981) Some thoughts about three neurons in the vestibulo-ocular reflex. In: Cohen B (ed) Vestibular and oculomotor physiology. Ann N Y Acad Sci 374:171–188

Baloh RW, Jacobson KM, Beukirch K, Honrubia V (1989) Horizontal vestibulo-ocular reflex after acute peripheral lesions. Acta Otolaryngol [Suppl] 468:323–327

Barnes GR (1980) Vestibular control of oculomotor and postural mechanisms. Clin Phys Physiol Meas 1:3–40

Brichta AM, Goldberg JM (2000) Responses to efferent activation and excitatory response-intensity relations of turtle posterior-crista afferents. J Neuropshysiol 83:1224–1242

Broussard DM, Bhatia JK, Jones GEG (1999) The dynamics of the vestibulo-ocular reflex after peripheral vestibular damage. I. Frequency-dependent asymmetry. Exp Brain Res 125:353–364

Chan VS, Shum DK, Lai CH (1999) Neural response sensitivity to bi-directional off-vertical axis rotations: a dimension of imbalance in the bilateral vestibular nuclei of cats after unilateral labyrinthectomy. Neuroscience 94:831–843

Chen-Huang C, McCrea RA, Goldberg JM (1997) Contribution of regularly and irregularly discharging vestibular-nerve inputs to the discharge of centralvestibular neurons in the alert squirrel monkey. Exp Brain Res 114:405–422

Curthoys IS, Halmagyi GM (1995) Vestibular compensation: a review of the oculomotor, neural, and clinical consequences of unilateral vestibular loss. J Vestib Res 5:67–107

Dieringer N (1995) 'Vestibular compensation': neural plasticity and its relations to functional recovery after labyrinthine lesions in frogs and other vertebrates. Prog Neurobiol 46:97–129

Galiana HL (1985) Commissural vestibular nuclear coupling: a powerful putative site for producing adaptive change. In: Berthoz A, Melvill Jones G (eds) Adaptive mechanisms in gaze control – facts and theories. Elsevier, Amsterdam, pp 327–339

Galiana HL (1991) A nystagmus strategy to linearize the vestibulo-ocular reflex. IEEE Trans Biomed Eng 38:532–543

Galiana HL, Outerbridge JS (1984) A bilateral model for central neural pathways vestibular ocular reflex. J Neurophysiol 51:210–241

Galiana HL, Smith HL, Katsarkas A (1995) Comparing linear and non-linear methods for the analysis of the vestibulo-ocular reflex. Acta Otolaryngol (Stockholm) 115:585–596

Goldberg JM, Fernandez C (1971) Physiology of peripheral neurons innervating semicircular canals of the squirrel monkey. I. Resting discharge and response to constant angular accelerations. J Neurophysiol 34:635–660

Hain TC, Fetter M, Zee DS (1987) Head-shaking nystagmus in unilateral peripheral vestibular lesions. Am J Otolaryngol 8:36–47

Henn V, Lang W, Hepp K, Büttner-Ennever JA (1982) The primate oculomotor system. II. Premotor sysytem. Hum Neurobiol 1:87–95

Hess K, Baloh RW, Honrubia V, Yee RD (1985) Rotational testing in patients with bilateral peripheral vestibular disease. Laryngoscope 95:85–88

Hullar TE, Minor LB (1999) High-frequency dynamics of regularly discharging canal afferents provide a linear signal for angular vestibuloocular reflexes. J Neurophysiol 82:2000–2005

Katsarkas A, Galiana HL, Smith HL (1995) Vestibulo-ocular reflex(VOR) biases in normal subjects and patients with compensated vestibular loss. Acta Otolaryngol (Stockholm) 115:476–483

Katsarkas A, Smith HL, Galiana HL (1998) Unexpected non-linearities in the VOR responses of patients with bilateral loss of peripheral vestibular function. Presented at the 20th Regular Meeting of the Barany Society; Wurzburg, Germany, Sept. 12th-15th

Lasker DM, Backous D, Lysakowski A, Davis GL, Minor LB (1999) Horizontal vestibuloocular reflex evoked by high acceleration rotation in squirrel monkey. II. responses after canal plugging. J Neurophysiol 82:1271–1285

Lasker DM, Hullar TE, Minor LB (2000) Horizontal vestibulooocular reflex evoked by high acceleration rotations in the squirrel monkey. III. responses after labyrinthectomy. J Neurophysiol 83:2482–2496

Laurutis VP, Robinson DA (1986) The vestibulo-ocular reflex during human sacccadic eye movements. J Neurophysiol 373:209–233

Li W, Correia MJ (1998) Recovery of semicircular canal primary afferent activity in the pigeon after streptomycin ototoxicity. J Neurophysiol 80:3297–3311

Marlinski V, Plotnik M, Goldberg JM (2000) Responses of vestibular nerve afferents to electrical stimulation of brainstem efferent pathways in anesthetized chinchillas. Soc Neurosci Abstr 78:1491

Mettens P, Godaux E, Cheron G, Galiana HL (1994) Effect of muscimol microinjections into the prepositus hypoglossi and the medial vestibular nuclei on cat eye movements. J Neurophysiol 72:785–802

Minor LB, Goldberg JM (1991) Vestibular-nerve inputs to the vestibulo-ocular reflex: a functional ablation study. J Neurosci 11:1636–1648

Minor LB, Lasker DM, Backous D, Hullar TE (1999) Horizontal vestibuloocular reflex evoked by high acceleration rotation in squirrel monkey. I. Normal responses. J Neurophysiol 82:1254–1270

Newlands SD, Perachio AA (1990) Compensation of horizontal canal related activity in the medial vestibular nucleus following unilateral labyrinth ablation in the decerebrate gerbil. I. Type I neurons. Exp Brain Res 82:359–372

Paige GD (1989) Nonlinearity and asymmetry in human vestibulo-ocular reflex. Acta Otolaryngol (Stockholm) 108:1–8

Raphan T, Cohen B, Matsuo V (1977) A velocity storage mechanism for optokinetic nystagmus (OKN) optokinetic after-nystagmus (OKAN) and vestibular nystagmus. In: Baker R, Berthoz A (eds) Control of gaze by brain stem neurons. Elsevier/North-Holland, Amsterdam, pp 37–47

Rey C, Galiana HL (1991) Parametric classification of segments in ocular nystagmus. IEEE Trans Biomed Eng 38:142–148

Scudder CA, Fuchs AF (1992) Physiological and behavioral identification of vestibular nucleus neurons mediating the horizontal vestibuloocular reflex in trained rhesus monkeys. J Neurophysiol 68:244–263

Segal BN, Outerbridge JS (1982) Vestibular (semicircular canal) primary neurons in bullfrog: nonlinearity of individual and population response to rotation. J Neurophysiol 47:545–562

Smith HLH, Galiana HL (1991) The role of structural symmetry in linearizing ocular reflexes. Biol Cybern 65:11–22

Smith HL, Galiana HL, Katsarkas A (1997) A bilateral VOR model explains non-linearities in unilateral and bilateral vestibularly deficient patients. Soc Neurosci Abstr 23:1293

Tomlinson RD, Bahra PS (1986) Combined eye-head gaze shifts in primates. I. Metrics. J Neurophysiol 56:1542–1557

Yamanaka T, Him A, Cameron SA, Dutia MB (2000) Rapid compensatory changes in GABA receptor efficacy in rat vestibular neurones after unilateral labyrinthectomy. J Physiol 523:413–424